2009

Warming of the Antarctic ice-sheet surface since the 1957 International Geophysical Year

Eric J. Steig
University of Washington

David P. Schneider
National Center for Atmospheric Research, Boulder, Colorado

Scott Rutherford
Roger Williams University, srutherford@rwu.edu

Michael E. E. Mann
Pennsylvania State University

Josefino C. Comiso
NASA Laboratory for Hydrospheric and Biospheric Sciences,

See next page for additional authors

Recommended Citation

Authors
Eric J. Steig, David P. Schneider, Scott Rutherford, Michael E. E. Mann, Josefino C. Comiso, and Drew T. Shindell

Warming of the Antarctic ice-sheet surface since the 1957 International Geophysical Year

Eric J. Steig[1], David P. Schneider[2], Scott D. Rutherford[3], Michael E. Mann[4], Josefino C. Comiso[5] & Drew T. Shindell[6]

Assessments of Antarctic temperature change have emphasized the contrast between strong warming of the Antarctic Peninsula and slight cooling of the Antarctic continental interior in recent decades[1]. This pattern of temperature change has been attributed to the increased strength of the circumpolar westerlies, largely in response to changes in stratospheric ozone[2]. This picture, however, is substantially incomplete owing to the sparseness and short duration of the observations. Here we show that significant warming extends well beyond the Antarctic Peninsula to cover most of West Antarctica, an area of warming much larger than previously reported. West Antarctic warming exceeds 0.1 °C per decade over the past 50 years, and is strongest in winter and spring. Although this is partly offset by autumn cooling in East Antarctica, the continent-wide average near-surface temperature trend is positive. Simulations using a general circulation model reproduce the essential features of the spatial pattern and the long-term trend, and we suggest that neither can be attributed directly to increases in the strength of the westerlies. Instead, regional changes in atmospheric circulation and associated changes in sea surface temperature and sea ice are required to explain the enhanced warming in West Antarctica.

Recent changes in Antarctic ice-sheet surface temperatures appear enigmatic when compared with global average temperature trends. Although the Antarctic Peninsula is one of the most rapidly warming locations on Earth, weather stations on the Antarctic continent generally show insignificant trends in recent decades[1]. However, all but two of the continuous records from weather stations are near the coast, providing little direct information on conditions in the continental interior. The widely used weather forecast reanalysis data are known to have errors owing to inconsistent assimilation skill in the satellite and pre-satellite eras[3].

In this Letter, we use statistical climate-field-reconstruction techniques to obtain a 50-year-long, spatially complete estimate of monthly Antarctic temperature anomalies. In essence, we use the spatial covariance structure of the surface temperature field to guide interpolation of the sparse but reliable 50-year-long records of 2-m temperature from occupied weather stations. Although it has been suggested that such interpolation is unreliable owing to the distances involved[1], large spatial scales are not inherently problematic if there is high spatial coherence, as is the case in continental Antarctica[4].

Previous reconstructions of Antarctic near-surface temperatures have yielded inconsistent results, particularly over West Antarctica, where records are few and discontinuous[5–7]. We improve upon this earlier work in several ways. We use two independent estimates of the spatial covariance of temperature across the Antarctic ice sheet: surface temperature measurements from satellite thermal infrared (T_{IR})
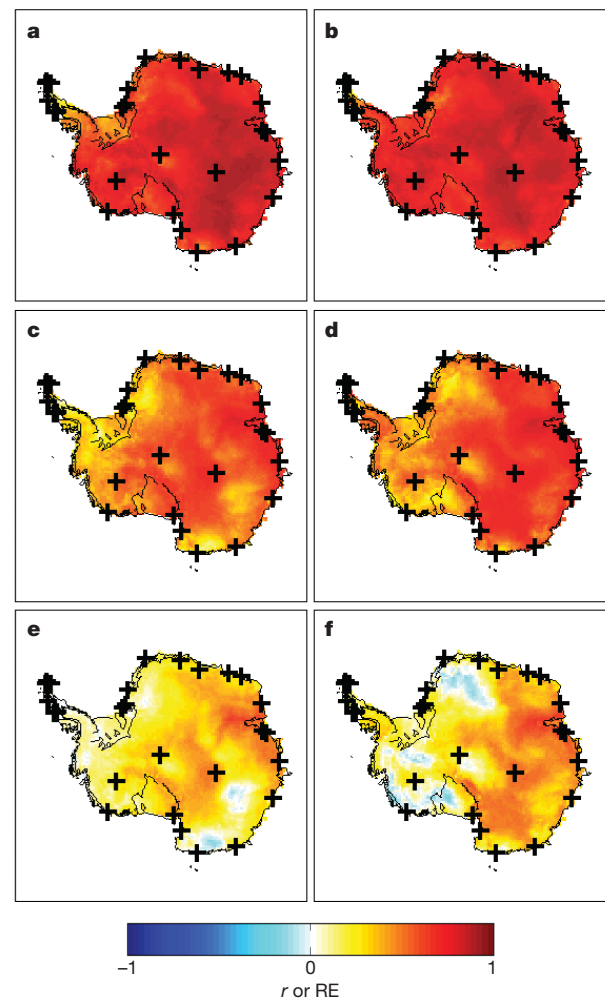

Figure 1 | Verification and upper-limit calibration statistics calculated for each grid point from the comparison of reconstructed and original satellite-derived monthly temperature anomalies. a, Calibration *r*, 1982–1994.5; **b**, calibration *r*, 1994.5–2006; **c**, verification *r*, 1994.5–2006; **d**, verification *r*, 1982–1994.5; **e**, verification RE, 1994.5–2006; **f**, verification RE, 1982–1994.5. Warm colours in **e** and **f** (RE scores greater than zero) show where results are more accurate than the climatological mean temperature. Mean grid-point verification results are RE = 0.11, CE = 0.09 and *r* = 0.46. Crosses show locations of occupied weather stations.

[1]Department of Earth and Space Sciences and Quaternary Research Center, University of Washington, Seattle, Washington 98195, USA. [2]National Center for Atmospheric Research, Boulder, Colorado 80307, USA. [3]Department of Environmental Science, Roger Williams University, Bristol, Rhode Island, USA. [4]Department of Meteorology, and Earth and Environmental Systems Institute, Pennsylvania State University, University Park, Pennsylvania 16802, USA. [5]NASA Laboratory for Hydrospheric and Biospheric Sciences, NASA Goddard Space Flight Center, Greenbelt, Maryland 20771, USA. [6]NASA Goddard Institute for Space Studies and Center for Climate Systems Research, Columbia University, New York, New York 10025, USA.

observations[8], and up-to-date automatic weather station (AWS) measurements of near-surface air temperature. We use a method[9,10] adapted from the regularized expectation maximization algorithm[11] (RegEM) for estimating missing data points in climate fields. RegEM is an iterative algorithm similar to principal-component analysis, used as a data-adaptive optimization of statistical weights for the weather station data. Unlike simple distance-weighting[5,6] or similar[7] calculations, application of RegEM takes into account temporal changes in the spatial covariance pattern, which depend on the relative importance of differing influences on Antarctic temperature at a given time. Furthermore, the iterative nature of RegEM allows it to be used with discontinuous time series, permitting us to take full advantage of the data available from occupied weather stations. We assess reconstruction skill using reduction-of-error (RE) and coefficient-of-efficiency (CE) scores as well as conventional correlation (r) scores. Such verification metrics are lacking in previous Antarctic temperature reconstructions[5–7], but are required for demonstrating skill relative to the climatological mean and are therefore critical for confidence in the calculation of temporal trends[10]. Skill metrics for our T_{IR}-based reconstruction from split calibration and verification experiments are significant (>99% confidence) at all grid points except in some restricted areas, mostly on the eastern side of the Antarctic Peninsula (Fig. 1).

Results from our AWS-based reconstruction agree well with those from the T_{IR} data (Fig. 2). This is important because the infrared data are strictly a measure of clear-sky temperature[8] and because surface temperature differs from air temperature 2–3 m above the surface, as measured at occupied stations or at AWSs. Trends in cloudiness or in the strength of the near-surface inversion could both produce spurious trends in the temperature reconstruction. The agreement between the reconstructions, however, rules out either potential bias as significant. Furthermore, detrending of the T_{IR} data before reconstruction demonstrates that the results do not depend strongly on trends in said data (Supplementary Information).

Our reconstructions show more significant temperature change in Antarctica (Fig. 2), and a different pattern for that change than reported in some previous reconstructions[5,7] (Fig. 3). We find that West Antarctica warmed between 1957 and 2006 at a rate of $0.17 \pm 0.06\,°C$ per decade (95% confidence interval). Thus, the area of warming is much larger than the region of the Antarctic Peninsula. The peninsula warming averages $0.11 \pm 0.04\,°C$ per decade. We also find significant warming in East Antarctica at $0.10 \pm 0.07\,°C$ per decade (1957–2006). The continent-wide trend is $0.12 \pm 0.07\,°C$ per decade. In the reconstruction based on detrended T_{IR} data, warming in West Antarctica remains significant at greater than 99% confidence, and the continent-wide mean trend remains at $0.08\,°C$ per decade, although it is no longer demonstrably different from zero (95% confidence). This is in good agreement with ref. 6, which reported average continent-wide warming of $0.082\,°C$ per decade (1962–2003) and shows overall warming in West Antarctica, although statistical significance could not be demonstrated owing to the shorter length and greater variance of the reconstruction. We emphasize that, in general,
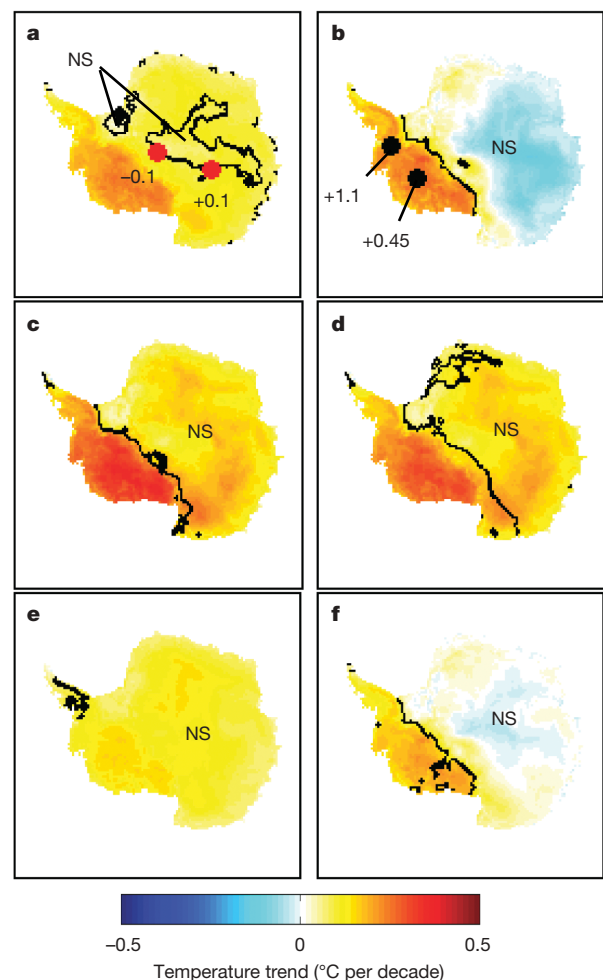
Figure 3 | Spatial pattern of temperature trends (degrees Celsius per decade) from reconstruction using infrared (T_{IR}) satellite data. a, Mean annual trends for 1957–2006; **b**, Mean annual trends for 1969–2000, to facilitate comparison with ref. 2. **c–f**, Seasonal trends for 1957–2006: winter (June, July, August; **c**); spring (September, October, November; **d**); summer (December, January, February; **e**); autumn (March, April, May; **f**). Black lines enclose those areas that have statistically significant trends at 95% confidence (two-tailed t-test). Where it would otherwise be unclear, NS (not significant) refers to areas of insignificant trends. Red circles and adjacent numbers in **a** show the locations of the South Pole and Vostok weather stations and their respective trends (degrees Celsius per decade) during the same time interval as the reconstruction (1957–2006). Black circles in **b** show the locations of Siple and Byrd Stations, and the adjacent numbers show their respective trends[13] for 1979–1997.
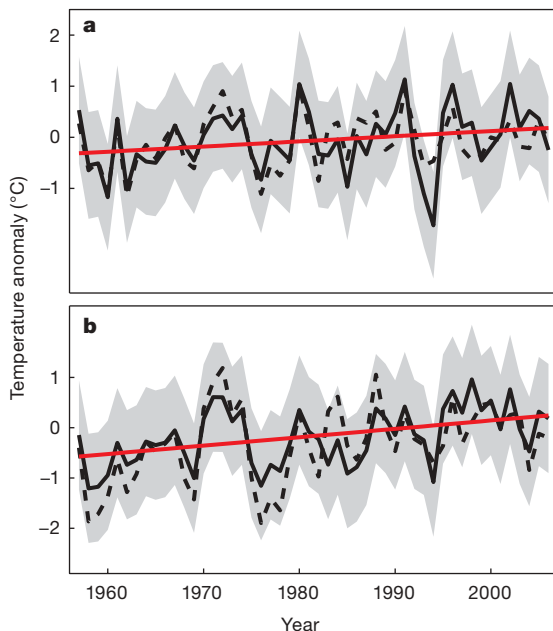
Figure 2 | Reconstructed annual mean Antarctic temperature anomalies, January 1957 to December 2006. a, East Antarctica; **b**, West Antarctica. Solid black lines show results from reconstruction using infrared satellite data, averaged over all grid points for each region. Dashed lines show the average of reconstructed AWS data in each region. Straight red lines show average trends of the T_{IR} reconstruction. Verification results for the continental mean of the T_{IR} reconstruction are RE = 0.34, CE = 0.31 and $r = 0.73$. Grey shading, 95% confidence limits.

detrending of predictand data lowers the quality of reconstructions by removing spatial covariance information[10]. The detrended reconstruction therefore represents a conservative lower bound on trend magnitude. Although ref. 7 concluded that recent temperature trends in West Antarctica are statistically insignificant, the results were strongly influenced by the paucity of data from that region. When the complete set of West Antarctic AWS data is included, the trends become positive and statistically significant, in excellent agreement with our results[12].

Independent data provide additional evidence that warming has been significant in West Antarctica. At Siple Station (76° S, 84° W) and Byrd Station (80° S, 120° W), short intervals of data from AWSs were spliced with 37-GHz (microwave) satellite observations, which are not affected by clouds, to obtain continuous records from 1979 to 1997 (ref. 13). The results show mean trends of 1.1 ± 0.8 °C per decade and 0.45 ± 1.3 °C per decade at Siple and Byrd, respectively[13]. Our reconstruction yields 0.29 ± 0.26 °C per decade and 0.36 ± 0.37 °C per decade over the same interval. In our full 50-year reconstruction, the trends are significant, although smaller, at both Byrd (0.23 ± 0.09 °C per decade) and Siple (0.18 ± 0.06 °C per decade). Furthermore, the seasonal characteristics of these data[13] agree well with those from our reconstructions, with the greatest amount of warming in austral spring and winter (Fig. 3). Independent analyses of tropospheric temperature trends have also found spring and winter warming to be greatest in West Antarctica[14,15].

The spatial and seasonal characteristics of our temperature reconstruction have important implications for understanding recent Antarctic climate change. Several studies have emphasized a warming-peninsula, cooling-continent pattern that is attributed to changes in atmospheric circulation associated with the southern annular mode (SAM)[2,16]. Cooling over much of East Antarctica did occur in recent decades, but was strongest during the short time interval considered in earlier studies (1969–2000; Fig. 3b). Virtually all areas warmed between 1957 and ~1980. Our reconstruction differs from the results of modelling experiments that tie Antarctic surface temperature change to stratospheric ozone loss through changes in the SAM[16–18]. In such simulations, the largest negative temperature anomalies in East Antarctica occur in summer, whereas in our reconstruction, East Antarctic cooling is restricted to autumn (Fig. 3). The simulations show warming in austral summer and autumn, restricted to the peninsula, whereas in our reconstruction the greatest warming is in winter and spring, and in continental West Antarctica as well as on the peninsula.

The well-known increases in temperature on the Antarctic Peninsula are strongly associated with changes in sea ice[19]. Similarly, negative anomalies in sea-ice extent[20] and the length of the sea-ice season[21] in the Amundsen–Bellingshausen Sea may be related to the warming trends we observe in adjacent West Antarctica. To explore this, we examined model output from the NASA Goddard Institute for Space Studies (GISS) ModelE atmosphere-only and coupled general circulation models, which were run with multiple oceanic and atmospheric boundary conditions until the end of 2003 (ref. 22). A slightly earlier atmospheric version of GISS ModelE has been used in simulations of circulation anomalies associated with polar stratospheric ozone depletion[17]. When driven by observed sea-surface-temperature (SST) and sea-ice boundary conditions[23], the model reproduces many of the basic features of our reconstruction, with warming over most of the continent and persistent in West Antarctica (Fig. 4). SST and sea-ice changes alone produced weak cooling over parts of East Antarctica during the 1980s and 1990s. The details of the comparisons obviously depend on the accuracy of the SST and sea-ice observations (the latter are not generally considered reliable before 1979), and multi-decadal internal variability in the model is substantial. However, it is noteworthy that both in the reconstruction and in the model results, the rate of warming is greater in continental West Antarctica, particularly in spring and winter, than either on the peninsula or in East Antarctica. In GISS ModelE, this is related to SST changes and the location of sea-ice anomalies, particularly during the latter period (1979–2003), when they are strongly zonally asymmetric, with significant losses in the West Antarctic sector but small gains around the rest of the continent (Fig. 4e). Radiative forcings alone are inadequate to account for the observations (Supplementary Information).

The net impact of SST, sea ice, and radiative forcings on Antarctic temperatures in GISS ModelE is in general agreement with our reconstruction. The same model, when run in coupled mode (that is, with a dynamic ocean) fails to reproduce the strong trends observed in West Antarctica and the peninsula. The probable cause of this discrepancy, common to other coupled models[24], is inadequate representation of sea-ice anomalies and their associated higher-order modes of
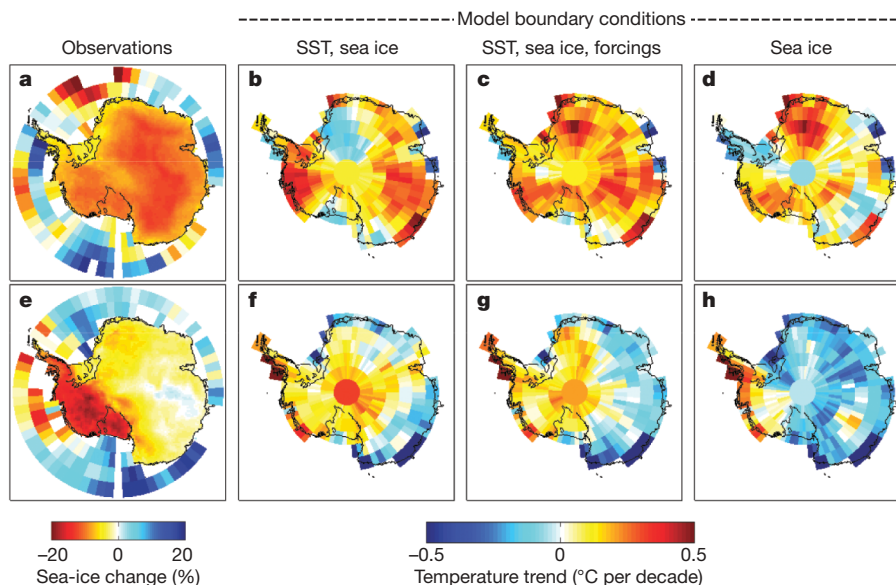

Figure 4 | Comparison of reconstructed and modelled mean annual temperature trends (degrees Celsius per decade) for the periods 1957–1981 and 1979–2003. a–d, 1957–1981; e–h, 1979–2003. a, e, Reconstructed surface temperature and observed 25-year change in sea-ice fractional area[23]. b, f, Surface air temperature from five-member GISS ModelE atmosphere-only ensemble simulations with observed sea-surface-temperature and sea-ice boundary conditions. c, g, Four-member ensemble with the same boundary conditions plus atmospheric forcings (changes in atmospheric concentrations of radiatively active species, including ozone). d, h, Difference between simulations with the same forcings but observed versus climatological sea ice, to isolate the effect of sea ice alone.

atmospheric circulation. In this context, it is important that the pattern of observed temperature trends closely resembles the pattern of temperature anomalies associated with the zonal wave-3 pattern in atmospheric circulation[4]. This circulation regime is efficient for the exchange of air between the ocean and the Antarctic continental interior, and is associated with atmospheric circulation anomalies in the Amundsen–Bellingshausen Sea, known to precede winter sea-ice anomalies[25]. Forced coupled models, including GISS ModelE, generally show a positive shift in the SAM and an associated increase in the circumpolar westerlies over recent decades, in good agreement with observations[26]. Observations also suggest a bias towards the positive phase in the wave-3 pattern[25] since about 1979, which is not reproduced in the coupled models. Using observed SST and sea ice, GISS ModelE does produce substantial shifts in the wave-3 circulation. Under those model conditions, greater cyclonic flow in the Amundsen Sea region brings warm, moist air to West Antarctica, countering the effect of the enhanced circumpolar westerlies.

An outstanding question in Antarctic climatology has been whether the strong warming of the peninsula has also occurred in continental West Antarctica[19]. Our results indicate that this is indeed the case, at least over the last 50 years. Moreover, ice-core analyses indicate average warming of West Antarctica over the entire twentieth century[27]. Although the influence of ozone-related changes in the SAM has been emphasized in recent studies of Antarctic temperature trends, the spatial and seasonal patterns of the observed temperature trends indicate that higher-order modes of atmospheric circulation, associated with regional sea-ice changes, have had a larger role in West Antarctica.

Mean surface temperature trends in both West and East Antarctica are positive for 1957–2006, and the mean continental warming is comparable to that for the Southern Hemisphere as a whole[28]. This warming trend is difficult to explain without the radiative forcing associated with increasing greenhouse-gas concentrations. However, the future trajectory of Antarctic temperature change also depends on the extent to which changes in atmospheric composition (whether from greenhouse gases or stratospheric ozone) affect Southern Hemisphere sea ice and regional atmospheric circulation patterns. Improved representation in models of coupled atmosphere/sea-ice dynamics will be critical for forecasting Antarctic temperature change.

METHODS SUMMARY

We use near-surface air temperature data from 42 occupied stations and 65 AWSs from the READER (Reference Antarctic Data for Environmental Research) data set[1]. We use passive infrared brightness measurements (T_{IR}) of surface temperature from the Advanced Very High Resolution Radiometer[8], a satellite of the US National Oceanic and Atmospheric Administration. We use the RegEM algorithm[9–11] to combine the data from occupied weather stations with the T_{IR} and AWS data in separate reconstructions of the near-surface Antarctic temperature field. Split calibration/verification tests are performed by withholding pre- and post-1995 T_{IR} and AWS data in separate RegEM calculations. Calibration and verification statistics are calculated for each grid point from the comparison of the reconstructed time series and the original temperature time series. We show RE and correlation r values in Fig. 1. CE verification values yield results indistinguishable from RE in our study and are reported in Supplementary Information. Significance levels of the calibration/verification statistics are based on Monte Carlo simulations of red noise as the null hypothesis. In Fig. 2, the 95% confidence interval is the unexplained variance, 2σ, where $\sigma^2_{error} = \sigma^2_{data}(1 - r^2_{ver})$, σ^2_{data} is the temporal variance in the original satellite temperature data and r^2_{ver} is the verification fractional resolved variance. Significance levels of trends are calculated using a two-tailed t-test, with the number of degrees of freedom adjusted for autocorrelation. In reporting trends for different areas, we define West Antarctica as $72°$–$90°$ S, $60°$–$180°$ W; East Antarctica as $65°$–$90°$ S, $300°$–$180°$ E; and the Antarctic Peninsula as westerly longitudes north of $72°$ S.

Full Methods and any associated references are available in the online version of the paper at www.nature.com/nature.

Received 14 January; accepted 1 December 2008.

1. Turner, J. et al. Antarctic climate change during the last 50 years. Int. J. Climatol. 25, 279–294 (2005).
2. Thompson, D. W. J. & Solomon, S. Interpretation of recent Southern Hemisphere climate change. Science 296, 895–899 (2002).
3. Bromwich, D. H. & Fogt, R. L. Strong trends in the skill of the ERA-40 and NCEP-NCAR Reanalyses in the high and midlatitudes of the southern hemisphere, 1958–2001. J. Clim. 17, 4603–4619 (2004).
4. Schneider, D. P., Steig, E. J. & Comiso, J. Recent climate variability in Antarctica from satellite-derived temperature data. J. Clim. 17, 1569–1583 (2004).
5. Doran, P. T. et al. Antarctic climate cooling and terrestrial ecosystem response. Nature 415, 517–520 (2002).
6. Chapman, W. L. & Walsh, J. E. A synthesis of Antarctic temperatures. J. Clim. 20, 4096–4117 (2007).
7. Monaghan, A. J., Bromwich, D. H., Chapman, W. & Comiso, J. C. Recent variability and trends of Antarctic near-surface temperature. J. Geophys. Res. 113, doi:1029/2007JD009094 (2008).
8. Comiso, J. C. Variability and trends in Antarctic surface temperatures from in situ and satellite infrared measurements. J. Clim. 13, 1674–1696 (2000).
9. Rutherford, S. et al. Proxy-based Northern Hemisphere surface temperature reconstructions: Sensitivity to methodology, predictor network, target season and target domain. J. Clim. 18, 2308–2329 (2005).
10. Mann, M. E., Rutherford, S., Wahl, E. & Ammann, C. Robustness of proxy-based climate field reconstruction methods. J. Geophys. Res. 112, doi:10.1029/2006JD008272 (2007).
11. Schneider, T. Analysis of incomplete climate data: Estimation of mean values and covariance matrices and imputation of missing values. J. Clim. 14, 853–871 (2001).
12. Bromwich, D. H., Monaghan, A. J. & Colwell, S. R. Surface and Mid-tropospheric Climate Change in Antarctica. Eos 89 (Fall meeting), abstr. C41A-0497 (2008).
13. Shuman, C. A. & Stearns, C. R. Decadal-length composite inland West Antarctic temperature records. J. Clim. 14, 1977–1988 (2001).
14. Johanson, C. M. & Fu, Q. Antarctic atmospheric temperature trend patterns from satellite observations. Geophys. Res. Lett. 34, doi:1029/2006GL029108 (2007).
15. Turner, J. et al. Significant warming of the Antarctic winter troposphere. Science 311, 1914–1917 (2006).
16. Gillett, N. P. & Thompson, D. W. J. Simulation of recent Southern Hemisphere climate change. Science 302, 273–275 (2003).
17. Shindell, D. T. & Schmidt, G. A. Southern Hemisphere climate response to ozone changes and greenhouse gas increases. Geophys. Res. Lett. 31, doi:10.1029/2004GL020724 (2004).
18. Keeley, S. P. E. et al. Is Antarctic climate most sensitive to ozone depletion in the middle or lower stratosphere? Geophys. Res. Lett. 34, doi:10.1029/2007GL031238 (2007).
19. Vaughan, D. G. et al. Recent rapid regional climate warming on the Antarctic Peninsula. Clim. Change 60, 243–274 (2003).
20. Kwok, R. & Comiso, J. C. Southern Ocean climate and sea ice anomalies associated with the Southern Oscillation. J. Clim. 15, 487–501 (2002).
21. Parkinson, C. L. Trends in the length of the Southern Ocean sea ice season, 1979–1999. Ann. Glaciol. 34, 435–440 (2002).
22. Hansen, J. et al. Climate simulations for 1880–2003 with GISS Model E. Clim. Dyn. 29, 661–696 (2007).
23. Rayner, N. A. et al. Global analyses of sea surface temperature, sea ice and night marine air temperatures since the late nineteenth century. J. Geophys. Res. 108, doi:10.1029/2002JD002670 (2003).
24. Connolley, W. M. & Bracegirdle, T. J. An Antarctic assessment of IPCC AR4 coupled models. Geophys. Res. Lett. 34, doi:10.1029/2007GL031648 (2007).
25. Holland, M. M. & Raphael, M. Twentieth century simulation of the Southern Hemisphere in coupled models. Part II: Sea ice conditions and variability. Clim. Dyn. 26, 229–245 (2006).
26. Miller, R. L., Schmidt, G. A. & Shindell, D. T. Forced annular variations in the 20th Century Intergovernmental Panel on Climate Change Fourth Assessment Report models. J. Geophys. Res. 111, doi:10.1029/2005JD006323 (2006).
27. Schneider, D. P. & Steig, E. J. Ice cores record significant 1940s Antarctic warmth related to tropical climate variability. Proc. Natl Acad. Sci. USA 105, 12154–12158 (2008).
28. Jones, P. D. & Moberg, A. Hemispheric and large-scale surface air temperature variations: An extensive revision and an update to 2001. J. Clim. 16, 206–223 (2003).

Author Contributions E.J.S., D.P.S., S.D.R. and M.E.M. made the reconstruction and statistical calculations. J.C.C. performed the cloud-masking calculations and provided the updated satellite data set. D.T.S. provided the general circulation model output and guided its interpretation. E.J.S. wrote the paper. All authors discussed the results and commented on the manuscript.

Author Information Reprints and permissions information is available at www.nature.com/reprints. Correspondence and requests for materials should be addressed to E.J.S. (steig@ess.washington.edu).

METHODS

Data. We use the READER weather station temperatures from the British Antarctic Survey[1]. Twenty-seven of the 42 occupied stations have at least 50%-complete monthly average data from 1957 to present. Data from 65 AWSs are available, but are discontinuous and date from 1980 at the earliest. In addition, data from only 24 of the AWSs are more than 50% complete for 1980–2006. We use passive infrared brightness measurements (T_{IR}) from the Advanced Very High Resolution Radiometer, which are continuous beginning January 1982 and constitute the most spatially complete Antarctic temperature data set. The T_{IR} data are biased towards clear-sky conditions, owing to the opacity of clouds in the infrared band. Cloud masking is probably the largest source of error in the retrieval of T_{IR} data from raw satellite spectral information. We have updated the data throughout 2006, using an enhanced cloud-masking technique to give better fidelity with existing occupied and automatic weather station data. We make use of the cloud masking in ref. 8 but impose an additional restriction that requires that daily anomalies be within a threshold of $\pm 10\,^{\circ}C$ of climatology, a conservative technique that will tend to damp extreme values and, hence, minimize trends[29]. Values that fall outside the threshold are removed.

Calculations. We use the RegEM algorithm[11], developed for sparse data infilling, to combine the occupied weather station data with the T_{IR} and AWS data in separate reconstructions of the Antarctic temperature field. RegEM uses an iterative calculation that converges on reconstructed fields that are most consistent with the covariance information present both in the predictor data (in this case the weather stations) and the predictand data (the satellite observations or AWS data). We use an adaptation of RegEM in which only a small number, k, of significant eigenvectors are used[10]. Additionally, we use a truncated total-least-squares (TTLS) calculation[30] that minimizes both the vector **b** and the matrix A in the linear regression model $A\mathbf{x} = \mathbf{b}$. (In this case A is the space-time data matrix, **b** is the principal component time series to be reconstructed and **x** represents the statistical weights.) Using RegEM with TTLS provides more robust results for climate field reconstruction than the ridge-regression method originally suggested in ref. 11 for data infilling problems, when there are large differences in data availability between the calibration and reconstruction intervals[10]. For completeness, we compare results from RegEM with those from conventional principal-component analysis (Supplementary Information).

Monthly average surface temperature anomalies were obtained from the T_{IR} data for the domain covering all land areas and ice shelves on the Antarctic continent, at 50 km $\times$ 50 km resolution[4]. The monthly anomalies are efficiently characterized by a small number of spatial weighting patterns and corresponding time series (principal components) that describe the varying contribution of each pattern. The results are reproducible using single-season, annual average and split-decade-length subsets of the data[4]. The first three principal components are statistically separable and can be meaningfully related to important dynamical features of high-latitude Southern Hemisphere atmospheric circulation, as defined independently by extrapolar instrumental data. The first principal component is significantly correlated with the SAM index (the first principal component of sea-level-pressure or 500-hPa geopotential heights for 20° S–90° S), and the second principal component reflects the zonal wave-3 pattern, which contributes to the Antarctic dipole pattern of sea-ice anomalies in the Ross Sea and Weddell Sea sectors[4,8]. The first two principal components of T_{IR} alone explain >50% of the monthly and annual temperature variabilities[4]. Monthly anomalies from microwave data (not affected by clouds) yield virtually identical results[4].

Principal component analysis of the weather station data produces results similar to those of the satellite data analysis, yielding three separable principal components. We therefore used the RegEM algorithm with a cut-off parameter $k = 3$. A disadvantage of excluding higher-order terms ($k > 3$) is that this fails to fully capture the variance in the Antarctic Peninsula region. We accept this trade-off because the Peninsula is already the best-observed region of the Antarctic.

Statistics. We obtained calibration/verification statistics by withholding the first and last 12.5 years of the 25-year T_{IR} data in separate RegEM calculations. We similarly split the AWS data into pre- and post-1995 data. Confidence levels are based on Monte Carlo simulations of red noise as the null hypothesis. For each grid point, 1,000 red noise series were generated to have the same mean, variance and lag-1 autocorrelation coefficient as the actual time series over the calibration period. Additional validation of the T_{IR}-based reconstruction was obtained by using the 15 occupied weather stations with the most complete data, reserving the other 27 for verification. Verification metrics at these sites are consistently significant at >99% confidence, with the exception of some sites at the tip of the Antarctic Peninsula and the three sites north of 55° S (Supplementary Information).

We report verification statistics as well as upper-bound calibration-interval statistics. The latter represent the maximum level of explained variance that could be expected in the reconstruction, given how much data variance is resolved over the calibration interval. We rely primarily on the RE statistic; the alternative verification statistic, CE, yields indistinguishable results in our study (Supplementary Information). For completeness, we also report correlation r values, but with the recognition that r is a deficient skill metric because it does not penalize the poor prediction of either means or variances[10].

29. Reynolds, R. W. *et al.* An improved *in situ* and satellite SST analysis for climate. *J. Clim.* **15**, 1609–1625 (2002).
30. Fierro, R. D., Golub, G. H., Hansen, P. C. & O'Leary, D. P. Regularization by truncated total least squares. *SIAM J. Sci. Comput.* **18**, 1223–1241 (1997).

CORRIGENDUM

Warming of the Antarctic ice-sheet surface since the 1957 International Geophysical Year

Eric J. Steig, David P. Schneider, Scott D. Rutherford,
Michael E. Mann, Josefino C. Comiso & Drew T. Shindell

Nature **457**, 459–462 (2009)

In this Letter, we reported trends on reconstructed temperature histories for different areas of the Antarctic continent. The confidence levels on the trends, as given in the text, did not take into account the reduced degrees of freedom in the time series due to autocorrelation. We report in Table 1 the corrected values, based on a two-tailed *t*-test, with the number of degrees of freedom adjusted for autocorrelation, using $N_{effective} = N(1 - r)/(1 + r)$, in which N is the sample size and r is the lag-1 autocorrelation coefficient of the residuals of the detrended time series. The median of r is 0.27, resulting in a reduction in the degrees of freedom from $N = 600$ to $N_{effective} = 345$ for the monthly time series.

We also include results of a further calculation that takes into account both the variance and the uncertainty in the reconstructed temperatures. We performed Monte-Carlo simulations of the reconstructed temperatures using a Gaussian distribution with variance equal to the unresolved variance from the split calibration/verification tests described in the paper. Confidence bounds were obtained by detrending each simulation and obtaining the lag-1 autocorrelation coefficient and variance of the residuals; a random realization of Gaussian noise having the same lag-1 autocorrelation coefficient and variance was then added to the trend, and a new trend was calculated. The 2.5th and 97.5th percentiles of the 10,000 simulated trends give the 95% confidence bounds. For the case of zero unresolved variance, this calculation converges on the same value as the two-tailed *t*-test, above. The 95% confidence minimum trend value is given by the 5th percentile values of the simulated trends, last row of Table 1.

The corrected confidence levels do not change the assessed significance of trends, nor any of the primary conclusions of the paper. We also note that there is a typographical error in Supplementary Table 1: the correct location of Automatic Weather Station 'Harry' is 83.0° S, 238.6° E. The position of this station on the maps in the paper is correct.

Table 1 | Corrected confidence levels on mean decadal temperature trends

	West Antarctica	East Antarctica	Antarctic Peninsula	All Antarctica
Trend (°C per decade)	0.18	0.10	0.11	0.12
95% CI of trend in mean reconstruction	±0.09	±0.10	±0.05	±0.10
95% CI of trend, accounting for unresolved variance in mean reconstruction	±0.12	±0.13	±0.07	±0.12
Minimum trend (95% confidence, accounting for unresolved variance in mean reconstruction)	0.08	−0.01	0.05	0.02

The confidence levels are shown over the period 1957–2006 for the reported surface temperatures based on satellite data. CI, confidence interval.